Low-temperature thermochronologic signature of range-divide migration and breaching in the North Cascades

Thibaud Simon-Labric[1,2,*], Gilles Y. Brocard[3], Christian Teyssier[4], Peter A. van der Beek[2], Peter W. Reiners[5], David L. Shuster[6,7], Kendra E. Murray[5], and Donna L. Whitney[4]

[1]INSTITUTE OF EARTH SURFACE DYNAMICS, UNIVERSITY OF LAUSANNE, CH-1015 LAUSANNE, SWITZERLAND
[2]ISTERRE, UNIVERSITÉ GRENOBLE-ALPES, F-38000 GRENOBLE, FRANCE
[3]DEPARTMENT OF EARTH AND ENVIRONMENTAL SCIENCES, UNIVERSITY OF PENNSYLVANIA, PHILADELPHIA, PENNSYLVANIA 19104, USA
[4]DEPARTMENT OF EARTH SCIENCES, UNIVERSITY OF MINNESOTA, MINNEAPOLIS, MINNESOTA 55455, USA
[5]DEPARTMENT OF GEOSCIENCES, UNIVERSITY OF ARIZONA, TUCSON, ARIZONA 85721, USA
[6]DEPARTMENT OF EARTH AND PLANETARY SCIENCE, UNIVERSITY OF CALIFORNIA, BERKELEY, CALIFORNIA 94720, USA
[7]BERKELEY GEOCHRONOLOGY CENTER, 2455 RIDGE ROAD, BERKELEY, CALIFORNIA 94707, USA

ABSTRACT

Physical and numerical simulations of the development of mountain topography predict that asymmetric distributions of precipitation over a mountain range induce a migration of its drainage divide toward the driest flank in order to equilibrate erosion rates across the divide. Such migration is often inferred from existing asymmetries, but direct evidence for the migration is often lacking. New low-temperature apatite cooling ages from a transect across the northern North Cascades range (Washington, NW USA) and from two elevation profiles in the Skagit River valley record faster denudation on the western, wetter side of the range and lower denudation rates on the lee side of the range. This difference has already been documented further south along another transect across the range; however, in the south, the shift from young cooling ages to older ages occurs across the modern drainage divide. Here, further north, the shift occurs along a range-transverse valley within the Skagit Gorge. It has been proposed that the upper Skagit drainage was once a part of the leeward side of the range but started to drain toward the western side of the range across the Skagit Gorge in Quaternary time. Age-elevation profiles along the former drainage and in the Skagit Gorge restrict the onset of Skagit Gorge incision to the last 2 m.y., in agreement with $^4He/^3He$ data for the gorge floor. Breaching of the range drainage resulted in its displacement 40 km further east into the dry side of the range. In the 2000-m-deep, V-shaped Skagit Gorge, river stream power is still high, suggesting that incision of the gorge is still ongoing. Several other similar events have occurred along the range during the Pleistocene, supporting the proposed hypothesis that the repeated southward incursions of the Cordilleran ice sheet during this period triggered divide breaching and drainage reorganization by overflow of ice-dammed lakes at the front of the growing ice sheet. Since these events systematically rerouted streams toward the wet side of the range and resulted in leeward migration of the divide, we propose that in fact the Cordilleran ice sheet advance essentially catalyzed the adjustment of the mountain chain topography to the current orographic precipitation pattern.

INTRODUCTION

Climate is thought to have a global effect on the erosion and topography of mountain ranges (e.g., Montgomery et al., 2001; Champagnac et al., 2012; Herman et al., 2013). Many characteristics of mountain topography are expected to vary with climate (Willett, 1999), notably the position of range drainage divides. Physical (Bonnet, 2009) and numerical (Roe et al., 2003; Anders et al., 2008; Castelltort et al., 2012; Goren et al., 2013) simulations predict that an asymmetric orographic precipitation pattern generates asymmetric topography and migration of drainage divides toward the drier flanks of mountain ranges. As topography approaches geomorphic steady state, divide migration results in a progressive decline in slope on the

wet side of an orogen and an increase in slope on its arid side. Such theoretical adjustment is difficult to document in natural systems due to the continuous erosion of the ridge crest during its migration. Divide migration is thought to occur by progressive, diffusive lateral slope retreat or in successive discrete jumps by capture of rivers across the drainage divide (Craw et al., 1999; Willett et al., 2014). Such river diversions should be difficult to achieve in deeply incised orogens (Bishop, 1995), but they can still occur in a variety of ways, such as groundwater capture (Brocard et al., 2011, 2012) or lake overflow (Riedel et al., 2007). Reconstructions of paleodrainage patterns generally rely on distal proxies, such as changes in the routing of river sediments sourced in specific areas (e.g., Craw et al., 1999; Stokes et al., 2002; Maher et al., 2007; Brocard et al., 2011; Prince et al., 2011; Andrews et al., 2012), and on phyloge-

netic models (e.g., Craw et al., 2007; Ruzzante et al., 2008; Zemlak et al., 2010). However, in certain circumstances, the incision of deep canyons associated with drainage reorganization can leave a detectable footprint in the record of low-temperature cooling ages (Flowers and Farley, 2012; Karlstrom et al., 2014).

During the Quaternary, the North Cascades (Washington State, northwest USA) were repeatedly occupied by local temperate glaciers that deeply sculpted the landscape (Mitchell and Montgomery, 2006). In addition, north of 48.5°N, the range was invaded by the southward-flowing Cordilleran ice sheet (Fig. 1; Clague, 1989; Hendy, 2009). The ice sheet blocked many north-draining valleys, initiating reversals of their drainages. Numerous deeply incised V-shaped gorges found throughout this glacial landscape have been interpreted as interfluves breached during the overspill of these ice-
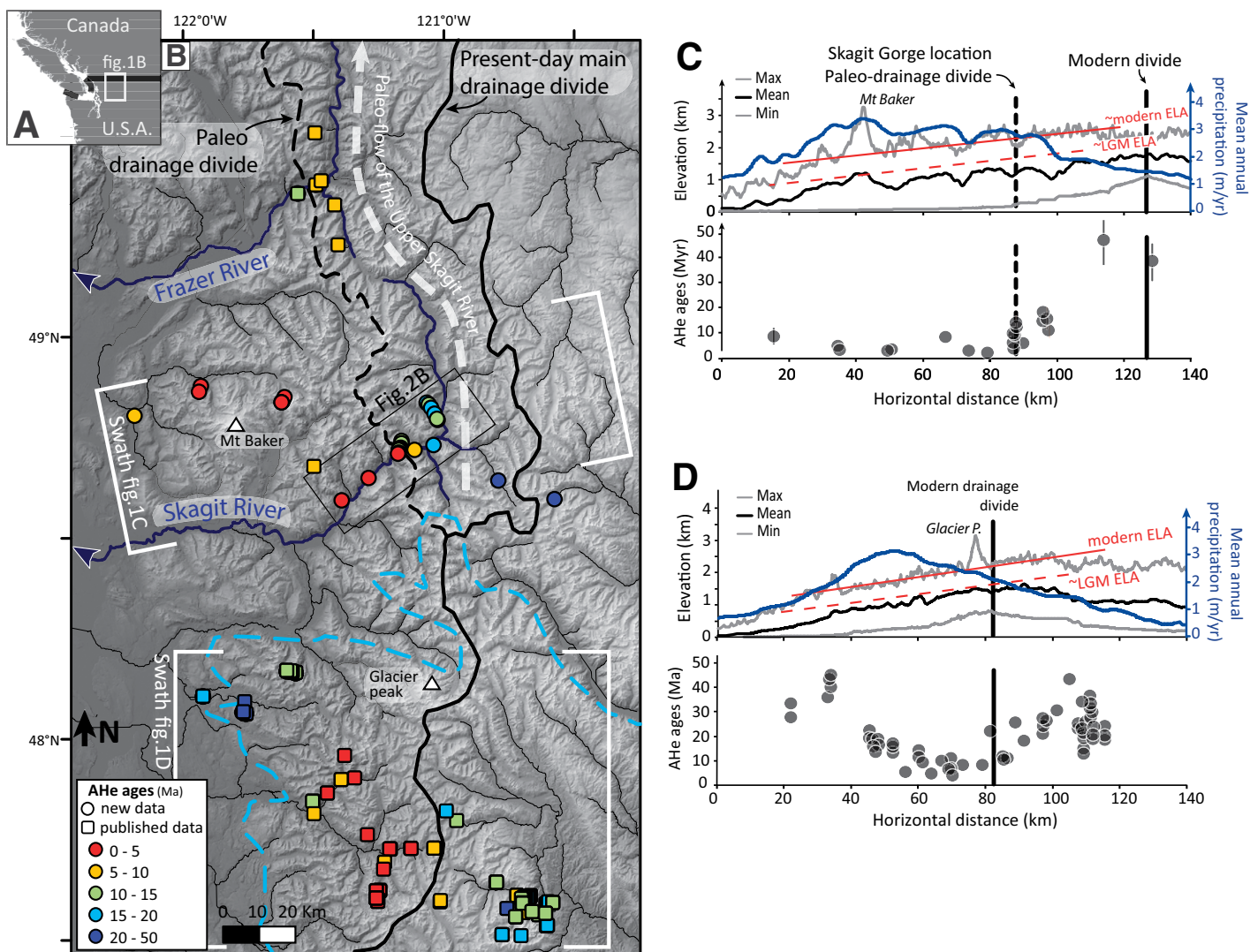
*thibaud.simon-labric@unil.ch

Figure 1. (A) Location of the northern Washington Cascades. (B) Shaded relief map showing present-day river network, present-day and paleo–drainage divides, and location of apatite (U-Th)/He (AHe) ages. Circles—new ages, squares—published ages (Reiners et al., 2002, 2003). Black arrows—present-day river flow direction; white dashed arrow—paleoflow direction; blue dashed line—southern extent of the latest Pleistocene advance of the Cordilleran ice sheet (south of the ice sheet, the range was occupied by locally fed valley glaciers). (C–D) Two east-west transects across the North Cascades at latitudes 47.5°N and 48.7°N, respectively (located on Fig. 1B). Apatite (U-Th)/He ages are shown as black circles with topographic profiles and mean annual precipitation profiles from 1960 to 1990 (http://www.ocs.orsu.edu/prism). Modern and Last Glacial Maximum (LGM) glacial equilibrium line altitudes (ELAs) are from Porter (1977).

dammed proglacial lakes that had formed at the front of the advancing ice sheet (Mathews et al., 1968; Riedel et al., 2007). One of them, the Skagit River Gorge, is a 2-km-deep, V-shaped section of the Skagit River valley, a 240-km-long range-transverse valley crossing the North Cascades. Riedel et al. (2007) proposed that the gorge formed during the Pleistocene by westward overspill of a proglacial lake, and this connected the modern upper drainage of the Skagit River to its lower course. Incision of the interfluve down to the elevation of surrounding valley floors allowed the permanent rerouting of the upper drainage through this gorge and a

definitive shift of the drainage divide 40 km to the east (Fig. 1).

In this study, we use low-temperature thermochronology to test this hypothesis and date the drainage adjustment. In the North Cascades, climate has been shown to strongly impact erosion patterns (Reiners et al., 2003). Orographic precipitation appears to drive enhanced erosion of the wet, windward side of the range over both intermediate- ($>10^4$ yr) and long-term ($>10^6$–10^7 yr) time scales, according to cosmogenic isotopes and apatite (U-Th)/He studies respectively (Fig. 1; Moon et al., 2011; Reiners et al., 2003). We present new low-temperature

thermochronology (apatite [U-Th]/He and ^{4}He/^{3}He) data collected along the Skagit River valley across the North Cascades and along two elevation profiles in and upstream (eastward) of the Skagit River Gorge (Fig. 1). The million-year denudation pattern is well correlated with the orographic precipitation pattern across the range. However, unlike in the southern part of the range at 47.5°N, where the transition from the young cooling ages of the western flank to the older ages of the eastern flank coincides with the position of the modern drainage divide, the transition here coincides with the Skagit Gorge location, supporting that the gorge corresponds

to the recent breaching of the range drainage divide. Age-elevation profiles along the Skagit Gorge, as well as ^{4}He/^{3}He data for the gorge floor, date the onset of gorge incision during the last 2 m.y. Finally, we propose that breaching of the preglaciation drainage divide, although triggered by glacial lake overspill, is fundamentally a long-term consequence of more rapid erosion of the wet side of the range. This breaching catalyzed drainage reorganization and forced long-term migration of the drainage divide toward the dry side of the range.

GEOLOGIC AND CLIMATIC SETTING

Geologic Evolution

The North Cascades range is the southern end of the >1200-km-long, 150-km-wide Coast Range that extends from SE Alaska through British Columbia (Canada) to Washington State (USA). Bedrock in the North Cascades is dominantly composed of high-grade metamorphic rocks intruded by Late Cretaceous to Eocene calc-alkaline plutons (Whitney et al., 1999; Miller et al., 2009). The North Cascades topography, which peaks at 3000 m, is supported by a buoyant crustal root; two-dimensional (2-D) seismic velocity profiles indicate crustal thicknesses of 35–40 km under central Washington (Schultz and Crosson, 1996). The North Cascades range has not been affected by significant internal deformation over the last 30–40 m.y.

Climatic Setting and Range-Scale Topography

The North Cascades currently block moisture influxes from the Pacific Ocean in the west. As a result, precipitation peaks at 5 m/yr over the western, windward side of the range but plummets down to 0.5 m/yr in its rain shadow to the east (Figs. 1C and 1D). Paleoclimate data indicate that this strong orographic precipitation gradient developed between 15 and 8 m.y. ago (Takeuchi and Larson, 2005).

The range was extensively glaciated during the Quaternary (Mitchell and Montgomery, 2006). Locally sourced mountain glaciers spread down the main valleys (Hendy, 2009). In addition, since at least the late Pleistocene (<600 k.y.), the Cordilleran continental ice sheet, centered over British Columbia, has repeatedly spread southward over the northern part of the Washington Cascades (Fig. 1; Waitt and Thorson, 1983; Clague, 1989). Deposits in the Puget Lowland indicate that the Cordilleran ice sheet has spread over the western piedmont of the Cascades at least six times since the middle Pleistocene (Easterbrook et al., 1988;

Booth et al., 2004). However, the marine isotope record suggests that these are but a fraction of the total ice sheet advances in the region during the last 2.5 m.y. (Booth et al., 2004). At its largest, the Cordilleran ice sheet reached elevations of more than 2000 m over much of its extent and a few nunataks protruded above it (Wilson et al., 1958; Clague, 1989).

Glacial erosion strongly shaped the topography of the Washington Cascades (Mitchell and Montgomery, 2006). Aside from Quaternary stratovolcanoes that stand above the regional topography, maximum and mean altitudes increase systematically from west to east (Figs. 1C and 1D), defining an inclined surface that correlates with the change in elevation of the local glacier equilibrium line altitude (ELA). The ELA rises 12 m/km toward the east (Porter, 1977) due to decreasing precipitation (e.g., Kuhn, 1989). In the Cascades, peaks and ridges stand on average 600 m above the ELA. This correlation suggests that glacial erosion has limited the height of the range, a process commonly referred to as the "glacial buzzsaw" (e.g., Brozović et al., 1997; Mitchell and Montgomery, 2006; Egholm et al., 2009).

Skagit River Drainage

The Skagit River crosscuts the highest ridges of the range (Fig. 1) along the 2000-m-deep, V-shaped Skagit Gorge, which connects the upper and lower U-shaped segments of the river (Figs. 2A and 2B). It has been proposed that the Skagit Gorge is a recent topographic feature resulting from the breaching of a paleodivide separating the upper and lower Skagit Rivers (Riedel et al., 2007). Originally, the paleo–upper Skagit River drained northward along a valley now occupied by the Ross Lake reservoir, whereas the current lower Skagit, already draining to the west into the Puget Sound, had its headwaters located in the vicinity of the Skagit Gorge (Fig. 1). Bedrock benches are found sporadically preserved along the upper Skagit River some 300–400 m above the modern river (Mathews, 1968; Haugerud, 1985). They have been interpreted as the relics of the U-shaped valley of the upper Skagit River before its connection to the lower Skagit River (Riedel et al., 2007). In particular, a 5-km-long bench above the southwest shore of Ross Lake dips in a direction opposite to the present-day flow direction of the Skagit River, suggesting flow reversal. In addition, the modern pass between the upper, south-flowing branch of the Skagit River and the upper, north-flowing branch of the Fraser River is a nice example of wind gap, which localizes the paleoflow of the upper Skagit (Fig. 1).

To explain this flow reversal, Riedel et al. (2007) proposed that a vast lake formed along

the ancestral upper Skagit when the Cordilleran ice sheet invaded its lower reaches. The ice dam grew and eventually overtopped a pass located at the current location of the Skagit Gorge. The lake waters spilled over the pass and cascaded down the west flank of the range, triggering rapid incision of the pass and drawdown of the lake. In effect, this event displaced the range drainage divide ~40 km further east (Fig. 1). Because lake overspill is an efficient way to overcome high-standing divides in deeply incised landscapes, it has been called upon to explain the abundance of valleys with a high degree of interconnectivity in ranges that were formerly occupied by ice sheets, such as in British Columbia (Kerr, 1936; Fulton, 1969), Scotland (Dury, 1953), and Scandinavia (Seuss, 1888).

GEOMORPHOLOGIC ANALYSIS OF THE SKAGIT RIVER PROFILE

We extracted the Skagit River profile from a 1 arc-second U.S. Geological Survey (USGS) National Elevation Data set (NED) digital elevation model (30 m grid resolution). Along the reaches currently flooded by the Ross Lake, Diablo, and Gorges reservoirs, we digitalized the profile from prereservoir 1:24,000 scale topographic maps elaborated in the 1930s. The river flows down a 200-m-high knick zone (reach of higher river gradient) as it passes the Skagit Gorge (Fig. 2C). The knick zone is unrelated to any active fault, lithological contact, or junction of overdeepened glacial valleys. The knick zone only coincides with the Skagit Gorge and with a 50% increase in the drainage area of the Skagit River. We calculated mean annual river power ω (W m^{-2}) for the Skagit River as a proxy for its fluvial erosive power using (Finlayson et al., 2002):

$$\omega = \frac{\rho g Q S}{W}, \qquad (1)$$

where ρ is the density of water (kg m^{-3}), g is gravitational acceleration (m s^{-2}), Q is fluvial discharge (m^3 s^{-1}), S is river slope, W is channel width (m), and k is a proportionality constant (kg m$^{-15/8}$ s$^{-19/8}$). To account for the spatial variability of precipitation in the Skagit basin, mean annual discharge Q was calculated from averaged annual precipitation data collected between 1960 and 1990 (http://www.ocs.orsu.edu/prism). The river channel width decreases as slope increases within the Skagit Gorge and knick zone. Because the reservoirs prevent any precise measurement of the channel width, we also estimated the stream power using an equation that incorporates an empirical calibration of the reduction in channel width with increasing channel slope (Finnegan et al., 2005):
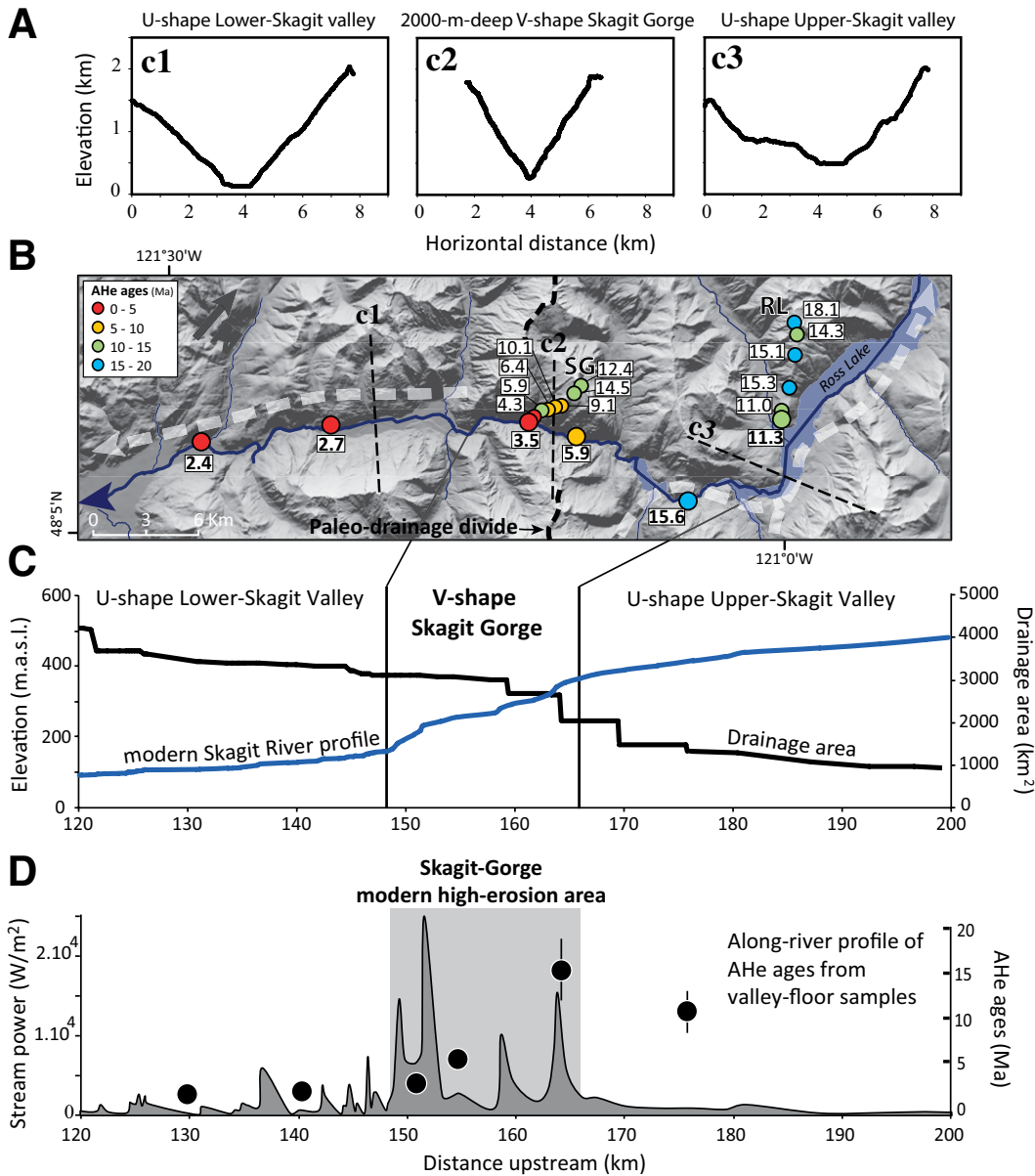
Figure 2. (A) Topographic cross section across the Skagit River, downstream (c1), in (c2), and upstream (c3) of the Skagit River Gorge. (B) Shaded topography of the Skagit River Gorge and location of the Skagit Gorge (SG) and Ross Lake (RL) thermochronological age-elevation profiles. AHe samples are indicated by their age (key as in Fig. 1). (C) River profile and evolution of drainage area along the Skagit River (m.a.s.l.—meters above sea level). (D) Comparison of unit stream power (W m⁻²) and AHe ages of valley-floor samples. Channel gradient was calculated by linear regression of the elevation profile over 500-m-long bins.

$$\omega = \frac{\rho g Q S}{W} \approx k Q^{5/8} S^{19/16}. \qquad (2)$$

The modeled unit stream power is not a direct measurement of river incision rate, but it is useful to estimate along-stream variations in erosive potential (Finlayson et al., 2002), assuming homogeneous bedrock erodibility and bed roughness. In the Skagit Gorge, the modeled stream power is about four times higher than along the rest of the river (Fig. 2D). This peak does not correlate with any obvious change in bedrock erodibility within the gorge, indicating that the knick zone likely experiences faster incision. No significant differential uplift has taken place along the gorge over the last ~40 m.y.,

so faster incision cannot be a consequence of enhanced rock uplift. We conclude that it is a transient erosive signal, the nature of which is discussed in the discussion section.

LOW-TEMPERATURE THERMOCHRONOLOGY

Two different thermochronometers were used to track the denudation history of the Skagit Gorge and its surroundings: the apatite (U-Th)/He (AHe) and the apatite ⁴He/³He systems. The AHe system records rock cooling through temperatures of 80–60 °C (Farley, 2000; Shuster et al., 2006) and thus typically records bedrock exhumation through the upper 2–4 km of the

crust. Apatite ⁴He/³He thermochronology is based on the mapping of the radiogenic ⁴He distribution within single apatite crystals using proton-induced ³He production and step-degassing experiments (Shuster and Farley, 2004; Shuster et al., 2004). This technique reveals rock cooling history below ~90 °C, the temperature at which ⁴He starts to accumulate in apatite crystals.

Twenty-three samples were collected along the Skagit River valley, across the North Cascades, and along two elevation profiles, one located in the Skagit River Gorge and the other one above Ross Lake (Fig. 1). The AHe analyses were performed at the University of Arizona, and the ⁴He/³He analyses where conducted at the Berkeley Geochronology Center. Between

TABLE 1. SUMMARIZING APATITE (U-Th)/HE AGES FROM SKAGIT RIVER GORGE
AND ROSS LAKE, NORTHERN WASHINGTON CASCADES

Sample	Easting (WGS-84)	Northing (WGS-84)	Elevation (m)	AHe age (Ma ± 1σ)
013D25	−120.6298	48.5743	1173	38.8 ± 7.8
013D27	−120.8371	48.6243	1033	43.7 ± 6.9
013D28	−121.0771	48.7167	628	15.7 ± 3.3
09CAS16	−121.9142	48.8797	350	3.4 ± 0.7
09CAS18	−121.9264	48.8639	854	4.8 ± 1.8
12Cas14	−121.32201	48.63378	142	2.3 ± 0.6
12Cas25	−121.39841	48.58596	116	2.7 ± 0.2
12Cas26	−122.20283	48.81322	73	8.7 ± 2.7
12Cas10	−121.17249	48.70697	280	5.9 ± 0.8
Skagit Gorge profile				
01-1	−121.1975	48.7287	1953	12.4 ± 2.7
01-2	−121.1981	48.7234	1758	14.5 ± 2.1
01-4	−121.2005	48.7123	1347	9.1 ± 1.3
01-7	−121.2083	48.70667	680	5.9 ± 0.6
01-6	−121.2072	48.7076	904	6.4 ± 0.6
01-5	−121.2041	48.7112	1155	10.1 ±1.4
02-1	−121.2092	48.6999	345	4.3 ±1.0
02-2	−121.2116	48.6973	241	3.5 ±0.8
Ross Lake profile				
03-1	−121.0988	48.8223	1967	18.1 ± 1.8
03-2	−121.0914	48.8182	1778	14.3 ± 1.4
03-3	−121.0828	48.8095	1617	15.1 ± 1.5
03-5	−121.0703	48.7946	1181	15.3 ± 4.7
04-1	−121.0595	48.7793	692	11.0 ± 2.2
04-2	−121.0612	48.7818	916	11.3 ± 2.0

Note: Details for (U-Th)/He (AHe) age determinations are provided in the GSA Data Repository (see text footnote 1).

Figure 3. (U-Th)/He (AHe) age-elevation plots for the Skagit Gorge and Ross Lake profiles. AHe ages are reported in Table 1. Dashed straight line—weighted linear regression through the AHe ages, as given by the inverse of the weighted least-squares regression (Williamson, 1968), where the variation in slope represents the 1 – σ error in the estimate. Dashed black box—apatite [4]He/[3]He sample. Weighted-mean, minimum (1σ), and maximum (1σ) estimates of age-elevation trend (denudation rate *E*) are indicated.

two and seven replicates of each samples were measured, with more replicates being measured along the elevation profiles. The results were used for quantitative thermal modeling. Most samples reproduced very well, and only a few grains were excluded from the calculation of average AHe ages. The sample-averaged AHe ages, corrected for α-ejection, are summarized in Table 1. The details of the applied corrections are provided as supplementary material (Tables DR1 and DR2 for AHe, and Table DR3 for apatite [4]He/[3]He).[1]

Spatial Variability of the AHe Ages Across the North Cascades

AHe ages were obtained on 11 bedrock samples collected over the width of the North Cascades orogen at the latitude of the Skagit River Gorge (48.7°N). Cooling ages range from 40 ± 0.8 Ma to 2.0 ± 0.8 Ma (Fig. 1; Table 1). Like further south at 47.5°N, the AHe ages display a U-shaped pattern, and the location of the youngest ages correlates with the maximum in

modern precipitation (Fig. 1C). However, unlike at 47.5°N, where the transition from the young ages of the western flank to the older ages of the eastern flank coincides with the position of the modern drainage divide, the transition here coincides with the Skagit Gorge, supporting the hypothesis that the Skagit Gorge results from the incision of the paleo–drainage divide.

Elevation Profiles

The Skagit Gorge (SG) profile and the Ross Lake (RL) profile were sampled ~15 km apart. The Ross Lake profile is located on the flank of the proposed ancestral valley of the north-flowing Skagit River (Fig. 2). Along both profiles, AHe ages correlate positively with elevation, yielding apparent long-term denudation rates of 0.1–0.2 km/m.y. between ca. 16 and 3 Ma (Fig. 3). However, the Skagit Gorge AHe ages are up to ~4 m.y. younger than those of the Ross Lake profile, implying faster recent denudation within the Skagit Gorge. Using the present-day geothermal gradient of ~25 °C/km (Blackwell et al., 1990), and extrapolating the AHe age-elevation trend to the present-day depth of the AHe closure temperature (~70 °C), the 3.5 Ma age at the bottom of the Skagit Gorge implies an increase of the denudation rate after
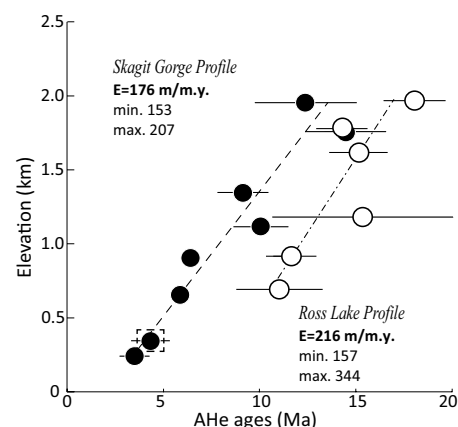
3 Ma in the Skagit Gorge at an average rate of ~900 m/m.y., while a steady and slower denudation rate (~200 m/m.y.) may have persisted in the Ross Lake area after 11 Ma.

To document this late-stage cooling history in more detail, we prepared samples from both profiles for [4]He/[3]He thermochronology. Only euhedral crystals free of visible mineral inclusions can be used for this technique (Shuster and Farley, 2004; Shuster et al., 2004). Only one crystal from the Skagit Gorge profile presented the required quality for [4]He/[3]He analysis; other apatites were polluted by minute zircon inclusions. Along the Ross Lake profile, all apatite crystals were either broken or noneuhedral. Valley-floor sample SG02-1 (345 m elevation) displays a diffusive [4]He-distribution pattern (Fig. 4A), which is typically produced by slow cooling through the partial retention zone and subsequent rapid cooling toward the topographic surface (Shuster et al., 2004). This result tends to support the analysis of the elevation-age trend; a more quantitative analysis of the cooling histories is presented next.

NUMERICAL MODELING OF TEMPERATURE-TIME PATHS

Thermal Inversion of the Apatite [4]He/[3]He Spectrum

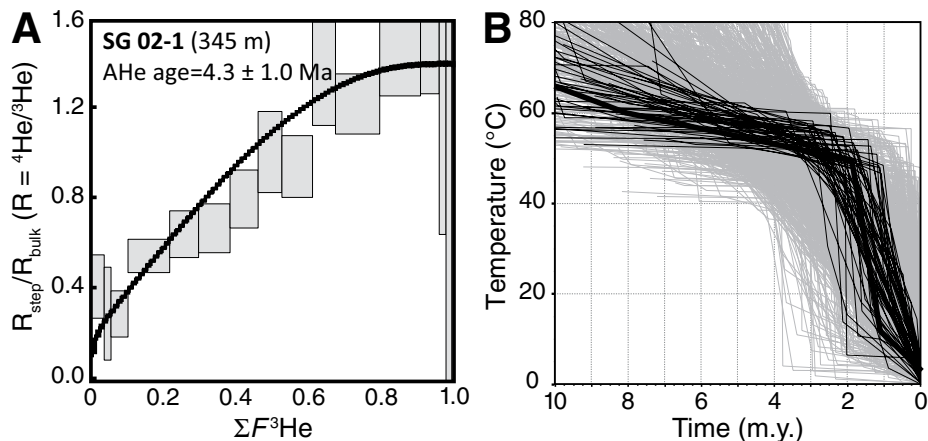To interpret the [4]He/[3]He results, we used a numerical model that predicts and inverts

Figure 4. (A) ^{4}He/^{3}He ratio evolution diagram for step-heating experiments of gorge-floor sample SG 02-1; plots show ^{4}He/^{3}He measurements of each step (R_{step}) normalized to the bulk ratio (R_{bulk}) determined by integrating all steps (open boxes: 1σ error) plotted against the cumulative ^{3}He release fraction (ΣF^3He). **(B)** Modeled cooling paths in time-temperature space. Black lines are cooling paths that show a good fit to the data, while dark- and light-gray lines show progressively worse fits that can be excluded at a 99% confidence level (Schildgen et al., 2010).

^{4}He distributions using a radiation-damage and annealing model to quantify He-diffusion kinetics in apatite (see Methods and supplementary information [see footnote 1]; Flowers et al., 2009). The model compares observed data to randomly generated temperature-time (T-t) histories; it explores a wide range of cooling histories and selects acceptable scenarios using a misfit-based evaluation. The misfit is defined as the mean of squared residuals weighted by the mean uncertainty in the ratio measurement (Schildgen et al., 2010). The input parameters include the characteristics of the analyzed crystal (apatite size, U and Th content) and its cooling history. The model carries the major assumption that U and Th are uniformly distributed within the analyzed apatite grain; this assumption is only challenged when an individual crystal possesses large concentric contrasts in the local concentration of U or Th (Farley et al., 2010). All cooling histories began at 150 °C and ended after 15 m.y. of simulation at the modern mean surface temperature (~5 °C). The model was able to reproduce the observed ^{4}He/^{3}He diffusion spectrum of apatite SG02-1 (Fig. 4A); it therefore adequately describes the He behavior in this apatite grain (Farley et al., 2011). The best-fit models produced gradual cooling through the AHe partial retention zone from ca. 10 to 2 Ma and faster cooling from ~50 °C to surface temperatures afterward (Fig. 4B). The initial slow cooling rate is poorly constrained between 0.6 and 4.5 °C/m.y., whereas the latter cooling rate is more tightly constrained between 20 and 25 °C/m.y.. The analysis of the ^{4}He/^{3}He profile requires a marked increase in cooling rate, consistent with the recent and rapid gorge incision scenario.

Thermal Inversion of Age-Elevation Profiles

The thermal history of the AHe age-elevation profiles was also simulated, this time using a transdimensional Markov chain Monte-Carlo inversion approach (Gallagher, 2012; see details in the Data Repository). The strength of this approach is its ability to use the spatial (elevation) relationship between samples to calculate T-t histories using all the samples in a profile. The expected models are presented for alpha-recoil damage models from Flowers et al. (2009). The modeling initiates with randomly chosen T-t paths and sets of kinetic parameters, for which a probability that the model fits the data is calculated. The parameter values are then slightly offset, and the probability of fitting the data is recalculated and compared to the initial model. The model with the highest probability is retained. This procedure is repeated 200,000 times (the number of iterations being chosen by the user), providing a large collection of models with their associated probabilities that allow model statistics to be calculated. A full explanation of the modeling procedure is provided in Gallagher (2012).

The Skagit Gorge and Ross Lake profiles were inverted separately with identical input parameters; cooling paths were randomly generated in a parameter space stretching 25 Ma to 0 Ma and by temperatures between 180 °C and 0 °C. No other constraints were imposed, allowing a full exploration of the range of statistically valuable models. The resulting best-fit thermal histories for the whole profiles are shown on Figure 5A and Figure 5B, together with the best-fit thermal histories of individual low-elevation samples (SG02-1 and RL04-1). In all cases, predicted T-t paths share a similar constant cooling rate of ~5 °C/m.y. from 15 to 3 Ma.

These inversion results provide accurate temporal evolution of cooling rates but cannot convert cooling rates into denudation rates. For this, it would be necessary to simulate the variation of the geothermal gradient as function of topography and its evolution through time (Braun et al., 2012). We consider that the geomorphological record is not sufficient to accurately reconstruct the paleotopography before the divide breaching and simulate its effect on the thermal structure. We therefore only propose an estimation of the denudation rates using a constant geothermal gradient of ~25 °C/km, based on heat-flow data mapping collected across the North Cascades (Blackwell et al., 1990). The cooling rate of ~5 °C/m.y. recorded by both elevation profiles then converts into a long-term denudation rate of ~200 m/m.y., consistent with the denudation rate inferred from the age-elevation trends. Slow cooling continues until today along the Ross Lake profile, whereas rapid cooling occurs after ca. 3 Ma in the lowermost samples of the Skagit Gorge profile at a rate of ~20 °C/m.y., as expected from the age-elevation trend.

To gain more insight on the recent episode of accelerated cooling, we added the ^{4}He/^{3}He spectrum of the gorge floor sample SG02-1 to the Skagit Gorge profile (Fig. 5C). The inversion confirms the need for a phase of substantial local cooling during the past 2 m.y. within the gorge, while maintaining steady cooling at higher elevation. Differential cooling between high- and low-elevation samples reaches ~40 °C. Importantly, the cooling pattern confirms the increase in denudation rate, but, in addition, it shows that faster cooling is restricted to the lowermost samples, implying relief growth through valley incision (e.g., Valla et al., 2011), rather than a widespread increase in erosion, with rapid incision of the gorge at a rate of ~800 m/m.y. during the past 2 m.y., superimposed onto a background denudation rate of ~200 m/m.y.

DISCUSSION

Breaching of the Drainage Divide by Proglacial Lake Overspill

The U-shaped pattern in the AHe ages that we observe at latitude 48.7°N is not correlated with the modern drainage divide but with the position of the Skagit Gorge, the modern divide

A Skagit Gorge age-elevation profile - 8 AHe ages

B Ross Lake age-elevation profile - 6 AHe ages

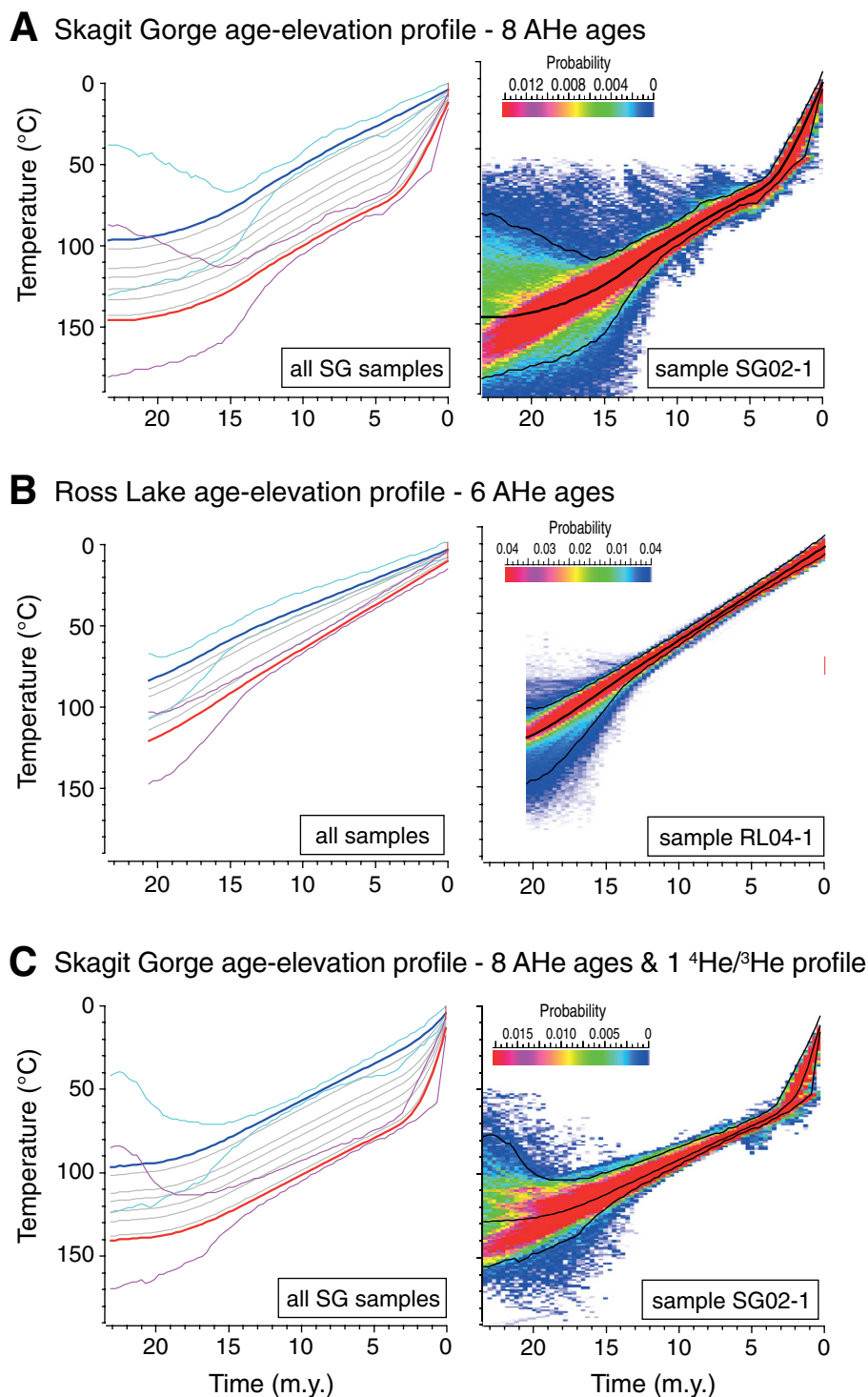# C Skagit Gorge age-elevation profile - 8 AHe ages & 1 ⁴He/³He profile

Figure 5. Thermal histories from inverse modeling of (A) Skagit Gorge (U-Th)/He (AHe) age-elevation profile, (B) Ross Lake AHe age-elevation profile, and (C) Skagit Gorge age-elevation profile and the ⁴He/³He spectrum of sample SG02-1. The inverse modeling (Gallagher, 2012) allows temperature-time (_T-t_) paths to be retrieved for a suite of vertically offset samples. For each model, left panels give the expected thermal history for the whole elevation profile, and right panels show expected thermal histories and the probability distribution for the lowest-elevation samples. On the left, thermal histories of the lowest- and highest-elevation samples are indicated by a red and blue thick line, respectively; intermediate-elevation samples are indicated by thin gray lines. The upper and lower thermal histories are shown together with their 95% confidence intervals. On the right, the expected (weighted mean) thermal history (thick black line) and the probability distribution for the lowest-elevation sample are indicated. The scale at the top indicates the probability.

being located ~40 km further east. However, the gorge crosscuts a topographic ridge that further south becomes the range drainage divide (Fig. 1). The denudation pattern and the map trajectory of the drainage divide together support Riedel et al.'s (2007) contention that the Upper Skagit basin was once part of the eastern flank of the range and was integrated to the west-flowing drainage through the Skagit Gorge (Fig. 5). The Skagit Gorge resulted from the incision of a low saddle that became the outflow channel of a proglacial lake that occupied the lower Skagit valley, bound to the north by the Cordilleran ice sheet.

According to this model, divide breaching and subsequent incision of the Skagit Gorge occurred during the Quaternary. This is confirmed by the thermochronology data in the Skagit Gorge and its surroundings. The cooling paths inferred from our age-elevation profiles indicate that between 15 and ca. 2 Ma, denudation of this part of the range was steady, uniform, and moderate at ~200 m/m.y. During the past ~2 m.y., substantial denudation occurred within the Skagit Gorge, while slow denudation continued in the Upper Skagit basin. The million-year resolution of thermochronological data does not allow us to date more precisely the initiation of gorge incision, but the incision of the Skagit Gorge could have started with the first arrival of the Cordilleran ice sheet in the area in Pleistocene time (Easterbrook et al., 1988; Booth et al., 2004). The distribution of stream power along the modern Skagit River further suggests that the period of rapid incision following the rerouting of the Skagit River across this ridge is still active. The thermal inversion of the Skagit Gorge profile also suggests that slow denudation persists at high elevations on the flanks of the gorge, resulting in a strong increase in local relief. The shoulders located at elevations at ~1800 m on either side of the gorge could be the remnants of the preexisting topography. In this case and considering that the shoulders are not eroding, the amount of incision since the overflow would reach a minimum of ~1500 m. Assuming a constant geothermal gradient of 25 °C/km, such incision would produce a maximum differential cooling of 37.5 °C between high- and low-elevation samples, close to the observed difference of 40 °C.

Quaternary Landward Migration of the Drainage Divide

Reiners et al. (2003) demonstrated that at 47.5°N, the minimum in AHe ages correlates spatially with the maximum intensity of precipitation, with the younger ages indicating greater denudation on the wet side of the orogen

(Figs. 1 and 2). Here at 48.7°N, this U-shaped pattern is also observed, but it is a little less pronounced, particularly in the west, where young AHe ages are obtained close to Mount Baker volcano (Haugerud and Tabor, 2009; Hildreth et al., 2003). These samples may have experienced magmatic heating, with partial or total age resetting. Heat-flow data collected across the Washington Cascades show that the regional geothermal gradient is significantly perturbed as far as ~10 km from active volcanic centers (Blackwell et al., 1990). Apart from this local perturbation, the similarity of the patterns at both latitudes leads us to conclude that the drainage divide used to pass through the Skagit River Gorge.

Numerical simulations of the impact of a migrating ridge on low-thermochronological ages (Olen et al., 2012) show broadly similar results to what we observe in our study area. Indeed, models predict synthetic AHe age-elevation relationships with similar slopes on either side of the migrating ridge, but younger on the retreating (windward) flank. Even under uniform rock uplift rate, the retreating flank of the ridge displays younger ages at a given elevation due to (1) the deformation of the isotherms below the topographic surface, which reduces the depth of the AHe closure temperature below the divide, and (2) focused erosion and increase in local relief in the wake of the migrating divide. Therefore, the ~4 m.y. shift in cooling ages from the Skagit Gorge to Ross Lake (Fig. 3) supports the contention that the Skagit Gorge was the main drainage divide before its breaching. Furthermore, comparison of our data set with published numerical simulations suggests that the divide was already migrating eastward before the breaching, but more data westward of the Skagit Gorge are necessary to confirm this hypothesis.

The breaching of the drainage divide by the Skagit River is not an isolated example. North of the Skagit River, the modern drainage divide is located east of the main summits; major rivers, such as the Fraser and Skeena Rivers, drain from east to west across the crest of the range. Drainage diversion and divide breaching by the Fraser River have been recently dated to <1.17 Ma based on the age of a lava flow that fills the abandoned precapture valley (Andrews et al., 2012). Against this backdrop, the diversion of the Skagit and Fraser Rivers no longer appears to be a random derangement of the drainage network during the invasion of the ice sheet, but rather a systematic westward breaching of the range divide along the entire range. We propose that the eastward migration of this divide during the Quaternary finds its place in a longer-term trend of migration that accelerated with proglacial lake overspill. This migration is fueled over the long term by the

asymmetric pattern of orographic precipitation that has characterized the range since the middle Miocene. The precipitation gradient has focused high long-term erosion rates on the humid side of the range and produced the formation of an asymmetric and inclined topography (Fig. 6A). This asymmetry explains the systematic rerouting of streams toward the humid side and the Pacific Ocean (Fig. 6). We have shown that, in the North Cascades, the retreat of the drainage divide, rather than progressive, occurred in discrete jumps due to diversion of rivers across the drainage divide. River diversion is very efficient in shifting the divide because it only requires the local erosion of an interfluve to produce instantaneous divide migration over a large distance. Similar stepwise breaching and leeward migration of the range drainage divide have been observed in the Patagonian Andes (Montgomery et al., 2001), where it also occurred during Quaternary times (Ruzzante et al., 2008; Zemlak et al., 2010). The Patagonian Andes also display an asymmetric long-term erosion pattern that correlates with orographic precipitation and glaciations (Thomson et al., 2010).

CONCLUSIONS

This study combined geomorphological analyses, inverse modeling of thermochronological

age-elevation profiles, and apatite ^{4}He/^{3}He thermochronology to evaluate the control exerted by precipitation on mountain range denudation rates and drainage divide dynamics. Analysis of denudation patterns in the northern Cascades range confirms earlier hypotheses suggesting that the Skagit River Gorge resulted from the breaching of a divide by the upper Skagit River. A range-transverse thermochronologic transect suggests that this ridge was the former range drainage divide. Cooling paths calculated using AHe age-elevation relationships on the flank of the gorge and a ^{4}He/^{3}He age on the gorge floor confirm an earlier hypothesis that the gorge formed within the past 2.0 m.y., likely by lake overflow. Anomalously high unit stream power in the 2000-m-deep Skagit River Gorge further suggests that rapid incision continues to present day within the breach. This river diversion occurred in a general context of range-scale drainage divide migration toward the leeward side of the range controlled by asymmetrical orographic precipitation. We suspect that this deep trend explains the systematic rerouting of ice-dammed streams toward the windward, humid side of the range during the Quaternary. Similar events have been documented all along the range during the Pleistocene. Thus, the incursions of the Cordilleran ice sheet would have simply catalyzed the drainage divide migration.
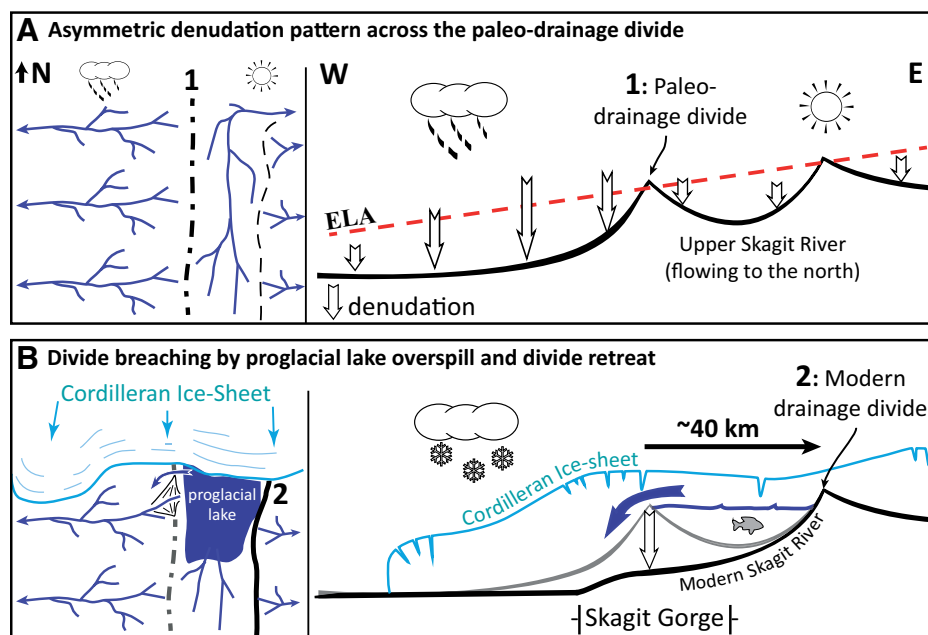

Figure 6. Conceptual sketch of the denudational and topographic evolution of the North Cascades derived from thermochronology data: (A) focused denudation (white arrows) on the windward side of the range. Orographic precipitation also controls the rise of the equilibrium line altitude (ELA) toward the arid flank and the formation of an inclined topography, such that maximum elevations are higher in the eastern part of the range. (B) Drainage divide breaching by proglacial lake overspill producing an instantaneous ~40 km eastward displacement of the drainage divide.

REFERENCES CITED

Anders, A.M., Roe, G.H., Montgomery, D.R., and Hallet, B., 2008, Influence of precipitation phase on the form of mountain ranges: Geology, v. 36, p. 479–482, doi: 10.1130/G24821A.1.

Andrews, G.D.M., Russell, J.K., Brown, S.R., and Enkin, R.G., 2012, Pleistocene reversal of the Fraser River, British Columbia: Geology, v. 40, p. 111–114, doi:10.1130/G32488.1.

Bishop, P., 1995, Drainage rearrangement by river capture, beheading and diversion: Progress in Physical Geography, v. 19, p. 449–473, doi:10.1177/030913339501900402.

Blackwell, D.D., Steele, J.L., Kelley, S., and Korosec, M.A., 1990, Heat flow in the state of Washington and thermal conditions in the Cascade Range: Journal of Geophysical Research, v. 95, p. 19,495–19,516, doi:10.1029/JB095iB12p19495.

Bonnet, S., 2009, Shrinking and splitting of drainage basins in orogenic landscapes from the migration of the main drainage divide: Nature Geoscience, v. 2, p. 766–771, doi:10.1038/ngeo666.

Booth, D.B., Troost, K.G., Clague, J.J., and Waitt, R.B., 2004, The Cordilleran ice sheet, *in* Gillespie, A.R., Porter, S.C., and Atwater, B.F., eds., The Quaternary Period in the U.S.: New York, Elsevier, Development in Quaternary Science, v. 1, p. 17–43.

Braun, J., Van Der Beek, P., Valla, P., et al., 2012, Quantifying rates of landscape evolution and tectonic processes by thermochronology and numerical modeling of crustal heat transport using PECUBE: Tectonophysics, v. 524, p. 1–28.

Brocard, G., Teyssier, C., Dunlap, W.J., Authemayou, C., Simon-Labric, T., Chiquín, L., Gutierrez, A., and Morán, S., 2011, Reorganization of a deeply incised drainage: Role of deformation, sedimentation and groundwater flow: Basin Research, v. 23, p. 631–651, doi:10.1111/j.1365-2117.2011.00510.x.

Brocard, G., Willenbring, J., Suski, B., et al., 2012, Rate and processes of river network rearrangement during incipient faulting: The case of the Cahabón River, Guatemala: American Journal of Science, v. 312, p. 449–507, doi:10.2475/05.2012.01.

Brozović, N., Burbank, D., and Meigs, A., 1997, Climatic limits on landscape development in the northwestern Himalaya: Science, v. 276, p. 571–574, doi:10.1126/science.276.5312.571.

Castelltort, S., Goren, L., Willett, S.D., Champagnac, J.-D., Herman, F., and Braun, J., 2012, River drainage patterns in the New Zealand Alps primarily controlled by plate tectonic strain: Nature Geoscience, v. 5, no. 10, p. 744–748, doi:10.1038/ngeo1582.

Champagnac, J.-D., Molnar, P., Sue, C., and Herman, F., 2012, Tectonics, climate, and mountain topography: Journal of Geophysical Research, v. 117, p. B02403, doi:10.1029/2011JB008348.

Clague, J.J., 1989, Development of Cordilleran landscapes during the Quaternary, *in* Fulton, R.J., ed., Quaternary Geology of Canada and Greenland: Geological Survey of Canada, Geology of Canada, v. K-1, p. 17–96.

Craw, D., Youngston, J.H., and Koons, P.O., 1999, Gold dispersal and placer formation in an active oblique collisonal mountain belt, Southern Alps, New Zealand: Economic Geology and the Bulletin of the Society of Economic Geologists, v. 94, p. 605–614, doi:10.2113/gsecongeo.94.5.605.

Craw, D., Burridge, C., Anderson, L., and Waters, J.M., 2007, Late Quaternary river drainage and fish evolution, Southland, New Zealand: Geomorphology, v. 84, p. 98–110, doi:10.1016/j.geomorph.2006.07.008.

Dury, G.H., 1953, A glacial breach in the north western highlands: Scottish Geographical Magazine, v. 69, p. 106–117, doi:10.1080/14702545308553799.

Easterbrook, D.J., Rowland, D.L., Carson, R.J., and Naeser, N.D., 1988, Application of fission-track dating, and tephra correlation to Lower Pleistocene sediments in

Puget Lowland, *in* Easterbrook, D.J., ed., Dating Quaternary Sediments: Geological Society of America Special Paper 227, p. 139–165.

Egholm, D.L., Nielsen, S.B., Pedersen, V.K., and Leseman, J.E., 2009, Glacial effects limiting mountain height: Nature, v. 460, p. 884–888, doi:10.1038/nature08263.

Farley, K.A., 2000, Helium diffusion from apatite: General behavior as illustrated by Durango fluorapatite: Journal of Geophysical Research, v. 105, p. 2903–2914, doi:10.1029/1999JB900348.

Farley, K.A., Shuster, D.L., Watson, E.B., Wanser, K.H., and Balco, G., 2010, Numerical investigations of apatite 4He/3He thermochronometry: Geochemistry, Geophysics, Geosystems, v. 11(10), Q10001, doi:10.1029/2010GC003243.

Farley, K.A., Shuster, D.L., and Ketcham, R.A., 2011, U and Th zonation in apatite observed by laser ablation ICPMS and implications for the (U-Th)/He system: Geochimica et Cosmochimica Acta, v. 75, p. 4515–4530, doi:10.1016/j.gca.2011.05.020.

Finlayson, D., Montgomery, D.R., and Hallet, B.H., 2002, Spatial coincidence of rapid inferred erosion with young metamorphic massifs in the Himalayas: Geology, v. 30, p. 219–222, doi:10.1130/0091-7613(2002)030<0219:SCORIE>2.0.CO;2.

Finnegan, N.J., Roe, G., Montgomery, D.R., and Hallet, B., 2005, A scaling relationship for channel width in bedrock rivers: Geology, v. 33, p. 229–232, doi:10.1130/G21171.1.

Flowers, R.M., and Farley, K.A., 2012, Apatite 4He/3He and (U-Th)/He evidence for an ancient Grand Canyon: Science, v. 338, p. 1616–1619, doi:10.1126/science.1229390.

Flowers, R.M., Ketcham, R.A., Shuster, D.L., and Farley, K.A., 2009, Apatite (U-Th)/He thermochronometry using a radiation damage accumulation and annealing model: Geochimica et Cosmochimica Acta, v. 73, p. 2347–2365, doi:10.1016/j.gca.2009.01.015.

Fulton, R.J., 1969, Glacial Lake History, Southern Interior Plateau, British Columbia: Geological Survey of Canada Paper 69–37, 14 p.

Gallagher, K., 2012, Transdimensional inverse thermal history modeling for quantitative thermochronology: Journal of Geophysical Research, v. 117, p. B02408, doi:10.1029/2011JB008825.

Goren, L., Willett, S.D., Herman, F., and Braun, J., 2013, Coupled numerical-analytical approach to landscape evolution modeling: Earth Surface Processes and Landforms, v. 39, no. 4, p. 522–545, doi:10.1002/esp.3514.

Haugerud, R.A., 1985, Geology of the Hozameen Group and the Ross Lake Shear Zone, Maselpanik Area, North Cascades, Southwestern British Columbia [Ph.D. thesis]: Seattle, Washington, University of Washington, 263 p.

Haugerud, R.A., and Tabor, R.W., 2009, Geologic Map of the North Cascade Range, Washington: U.S. Geological Survey Scientific Investigations Map 2940, 2 sheets, scale 1:200,000; 2 pamphlets, 29 p. and 23 p., http://pubs.usgs.gov/sim/2940/.

Hendy, I., 2009, A fresh perspective on the Cordilleran ice sheet: Geology, v. 37, p. 95–96, doi:10.1130/focus012009.1.

Herman, F., Seward, D., Valla, P.G., Carter, A., Kohn, B., Willett, S.D., and Ehlers, T.A., 2013, Worldwide acceleration of mountain erosion under a cooling climate: Nature, v. 504, p. 423–426, doi:10.1038/nature12877.

Hildreth, W., Fierstein, J., and Lanphere, M., 2003, Eruptive history and geochronology of the Mount Baker volcanic field, Washington: Geological Society of America Bulletin, v. 115, no. 6, p. 729–764, doi:10.1130/0016-7606(2003)115<0729:EHAGOT>2.0.CO;2.

Karlstrom, K.E., Lee, J.P., Kelley, S.A., Crow, R.S., Crossey, L.J., Young, R.A., Lazear, G., Beard, L.S., Ricketts, J.W., Fox, M., and Shuster, D.L., 2014, Formation of the Grand Canyon 5 to 6 million years ago through integration of older palaeocanyons: Nature Geoscience, v. 7, p. 239–244, doi:10.1038/ngeo2065.

Kerr, F.A., 1936, Quaternary glaciation in the Coast Range, northern British Columbia and Alaska: The Journal of Geology, v. 44, p. 681–700, doi:10.1086/624470.

Kuhn, M., 1989, The response of the ELA to climate fluctuations: Theory and observations, *in* Oerlemans, J., ed., Glacier Fluctuations and Climatic Change: Dordrecht, Netherlands, Kluwer, p. 407–417.

Maher, E., Harvey, A.M., and France, D., 2007, The impact of a major Quaternary river capture on the alluvial sedi-

ments of a beheaded river system, the Rio Alias, SE Spain: Geomorphology, v. 84, p. 344–356, doi:10.1016/j.geomorph.2005.07.034.

Mathews, W.H., 1968, Geomorphology of the Lightning Creek valley, Manning Park, southwest B.C.: Syesis, v. 1, p. 65–78.

Miller, R.B., Paterson, S.R., and Matzel, J.P., 2009, Plutonism at different crustal levels: Insights from the ~5–40 km (paleodepth) North Cascades crustal section, Washington, *in* Miller, R.B., and Snoke, A.W., eds., Crustal Cross Sections from the Western North American Cordillera and Elsewhere: Implications for Tectonic and Petrologic Processes: Geological Society of America Special Paper 456, p. 125–149, doi:10.1130/2009.2456(05).

Mitchell, S.G., and Montgomery, D.R., 2006, Influence of a glacial buzzsaw on the height and morphology of the Cascade Range in central Washington State, USA: Quaternary Research, v. 65, p. 96–107, doi:10.1016/j.yqres.2005.08.018.

Montgomery, D.R., Balco, G., and Willett, S.D., 2001, Climate, tectonics and the morphology of the Andes: Geology, v. 29, p. 579–582, doi:10.1130/0091-7613(2001)029<0579:CTATMO>2.0.CO;2.

Moon, S., Chamberlain, P.C., Blisniuk, K., Levine, N., Rodd, D.H., and Hilley, G.E., 2011, Climatic control of denudation in the deglaciated landscape of the Washington Cascades: Nature Geoscience, v. 4, p. 469–473, doi:10.1038/ngeo1159.

Olen, S.M., Ehlers, T.A., and Densmore, M.S., 2012, Limits to reconstructing paleotopography from thermochronometry data: Journal of Geophysical Research: Earth Surface (2003–2012), v. 117(F1), doi:10.1029/2011JF001985.

Porter, S.C., 1977, Present and past glaciation threshold in the Cascade Range, Washington, U.S.A.: Topographic and climatic controls, and paleoclimate implications: Journal of Glaciology, v. 18, p. 101–116.

Prince, P.S., Spotila, J.A., and Henika, W.S., 2011, Stream capture as driver of transient landscape evolution in a tectonically quiescent setting: Geology, v. 39, p. 823–826, doi:10.1130/G32008.1.

Reiners, P.W., Ehlers, T.A., Garver, J.I., Mitchell, S.G., Montgomery, D.R., Vance, J.A., and Nicolescu, S., 2002, Late Miocene exhumation and uplift of the Washington Cascade Range: Geology, v. 30, p. 767–770, doi:10.1130/0091-7613(2002)030<0767:LMEAUO>2.0.CO;2.

Reiners, P.W., Ehlers, T.A., Mitchell, S.G., and Montgomery, D.R., 2003, Coupled spatial variations in precipitation and long-term erosion rates across the Washington Cascades: Nature, v. 426, p. 645–647, doi:10.1038/nature02111.

Riedel, J.L., Haugerud, R.A., and Clague, J.J., 2007, Geomorphology of a Cordilleran ice sheet drainage network through breached divides in the North Cascades Mountains of Washington and British Columbia: Geomorphology, v. 91, p. 1–18, doi:10.1016/j.geomorph.2007.01.021.

Roe, G.H., Montgomery, D.R., and Hallet, B., 2003, Orographic precipitation and the relief of mountain ranges: Journal of Geophysical Research, v. 108, p. 2315, doi:10.1029/2001JB001521.

Ruzzante, D.E., Walde, S.J., Gosse, J.C., Cussac, V.E., Habit, E., Zemlak, T.S., and Adams, E.D.M., 2008, Climate control on ancestral population dynamics: Insight from Patagonian fish phylogeography: Molecular Ecology, v. 17, p. 2234–2244, doi:10.1111/j.1365-294X.2008.03738.x.

Schildgen, T.F., Balco, G., and Shuster, D.L., 2010, Canyon incision and knickpoint propagation recorded by apatite 4He/3He thermochronometry: Earth and Planetary Science Letters, v. 293, p. 377–387, doi:10.1016/j.epsl.2010.03.009.

Schultz, A.P., and Crosson, R.S., 1996, Seismic velocity structure across the central Washington Cascade range from refraction interpretation with earthquake sources: Journal of Geophysical Research, v. 101, p. 899–916, doi:10.1029/96JB02289.

Seuss, E., 1888, The Face of the Earth 2 (translated by Sollas, H.B.C., 1906): Oxford, UK, Clarendon Press, p. 326–345.

Shuster, D.L., and Farley, K.A., 2004, 4He/3He thermochronometry: Earth and Planetary Science Letters, v. 217, no. 1, p. 1–17, doi:10.1016/S0012-821X(03)00595-8.

Shuster, D.L., Farley, K.A., Sisterson, J.M., and Burnett, D.S., 2004, Quantifying the diffusion kinetics and spatial distributions of radiogenic 4He in minerals containing pro-

ton-induced ³He: Earth and Planetary Science Letters, v. 217, p. 19–32, doi:10.1016/S0012-821X(03)00594-6.

Shuster, D.L., Flowers, R.M., and Farley, K.A., 2006, The influence of natural radiation damage on helium diffusion kinetics in apatite: Earth and Planetary Science Letters, v. 249, no. 3, p. 148–161, doi:10.1016/j.epsl.2006.07.028.

Stokes, M., Mather, A.E., and Harvey, A.M., 2002, Quantification of river-capture–induced base-level changes and landscape development, Sorbas Basin, southeastern Spain, *in* Jones, S.J., and Frostick, L.E., eds., Sediment Flux to Basins: Causes, Controls and Consequences: Geological Society of London Special Publication 191, p. 23–35.

Takeuchi, A., and Larson, P.B., 2005, Oxygen isotope evidence for the late Cenozoic development of an orographic rain shadow in eastern Washington, USA: Geology, v. 33, p. 313–316, doi:10.1130/G21335.1.

Thomson, S.N., Brandon, M.T., Reiners, P.W., Tomkin, H., Vazquez, C., and Wilson, N., 2010, Glaciation as a destructive and constructive control on mountain building: Nature, v. 467, p. 313–317, doi:10.1038/nature09365.

Valla, P., Shuster, D.L., and van der Beek, P.A., 2011, Significant increase in relief of the European Alps during mid-Pleistocene glaciations: Nature Geoscience, v. 4, p. 688–692, doi:10.1038/ngeo1242.

Waitt, R.B., Jr., and Thorson, R.M., 1983, The Cordilleran ice sheet in Washington, Idaho, and Montana, *in* Porter, S.C., ed., Late-Quaternary Environments of the United States. The Late Pleistocene, Volume 1: Minneapolis, Minnesota, University of Minnesota Press, p. 54–70.

Whitney, D.L., Miller, R.B., and Paterson, S.R., 1999, *P-T-t* constraints on mechanisms of vertical tectonic motion in a contractional orogen: Journal of Metamorphic Geology, v. 17, p. 75–90, doi:10.1046/j.1525-1314.1999.00181.x.

Willett, S.D., 1999, Orogeny and orography: The effects of erosion on the structure of mountain belts: Journal of Geophysical Research–Solid Earth (1978–2012), v. 104, no. B12, p. 28,957–28,981.

Willett, S.D., McCoy, S.W., Perron, J.T., Goren, L., and Chen, C.Y., 2014, Dynamic reorganization of river basins: Science, v. 343, no. 6175, p. 1248765, doi:10.1126/science.1248765.

Williamson, J.H., 1968, Least squares fitting of a straight line: Canadian Journal of Physics, v. 46, p. 1845–1847, doi: 10.1139/p68-523.

Wilson, J.T., Falconer, G., Mathews, W.H., and Prest, V.K., compilers, 1958, Glacial Map of Canada: Toronto, Ontario, Canada, Geological Association of Canada, scale 1:3,801,600.

Zemlak, T.S., Habit, E.M., Walde, S.J., Carrea, C., and Ruzzante, D.E., 2010, Surviving historical Patagonian landscapes and climate: Molecular insights from *Galaxias maculatus*: BMC Evolutionary Biology, v. 10, p. 67, doi: 10.1186/1471-2148-10-67.